Formation and acceleration of uniformly filled ellipsoidal electron bunches obtained via space-charge-driven expansion from a cesium-telluride photocathode

P. Piot, Y.-E Sun, T.J. Maxwell, J. Ruan E. Secchi and J.C.T. Thangaraj

PRST-Accel. Beams 16, 010102 (2013)

(Received 10 October 2012; published 22 January 2013)

We report the experimental generation, acceleration and characterization of a uniformly filled electron bunch obtained via space-charge-driven expansion ("blow-out regime") in an L-band (1.3 GHz) rf photoinjector. The beam is photoemitted from a Cs2Te photocathode using short (< 200 fs) ultraviolet laser pulse. The produced electron bunches are characterized with conventional diagnostics and signatures of their ellipsoidal character are observed. We especially demonstrate the production of ellipsoidal bunches with charges up to ~0.5 nC corresponding to a ~20-fold increase compared to previous experiments with metallic photocathodes.

Martin Khojoyan
PITZ Physics Seminar
10.04.2014

Content

Introduction

Issues while creating 3D ellipsoidal beams via “blow-out” regime

- In theoretical astrophysics it has been realized that a uniform prolate spheroid will collapse under its own weight into a flat disk with the following density distribution: $\rho(r,z) = \sigma_0 \sqrt{1-(r/R)^2}\,\delta(z)$
- Reversing this collapsing process implies that an ultrathin sheet (with finite thickness) of electrons with a mentioned charge density distribution will evolve into a uniformly charged spheroid
- In a pancake regime (bunch length << bunch radius) the intensity profile of the laser pulse has to be shaped only transversely (the temporal shape is arbitrary) to a half-circular profile which will result to a 3D ellipsoidal electron bunches after the emission.

$$\frac{eE_{acc} c \tau_l}{mc^2} << \frac{\sigma_0}{\varepsilon_0 E_{acc}} << 1$$

, where $\sigma_0 \equiv \frac{Q}{\pi r^2}$ is the initial surface charge density, τ_l is the duration of photoemission process.

- Laser pulse length should be much smaller than the final bunch length
- The ratio of surface charge field and the acceleration field should be much smaller than 1

Assumption: the photoemission process is instantaneous !

Region of existence of blow-out regime

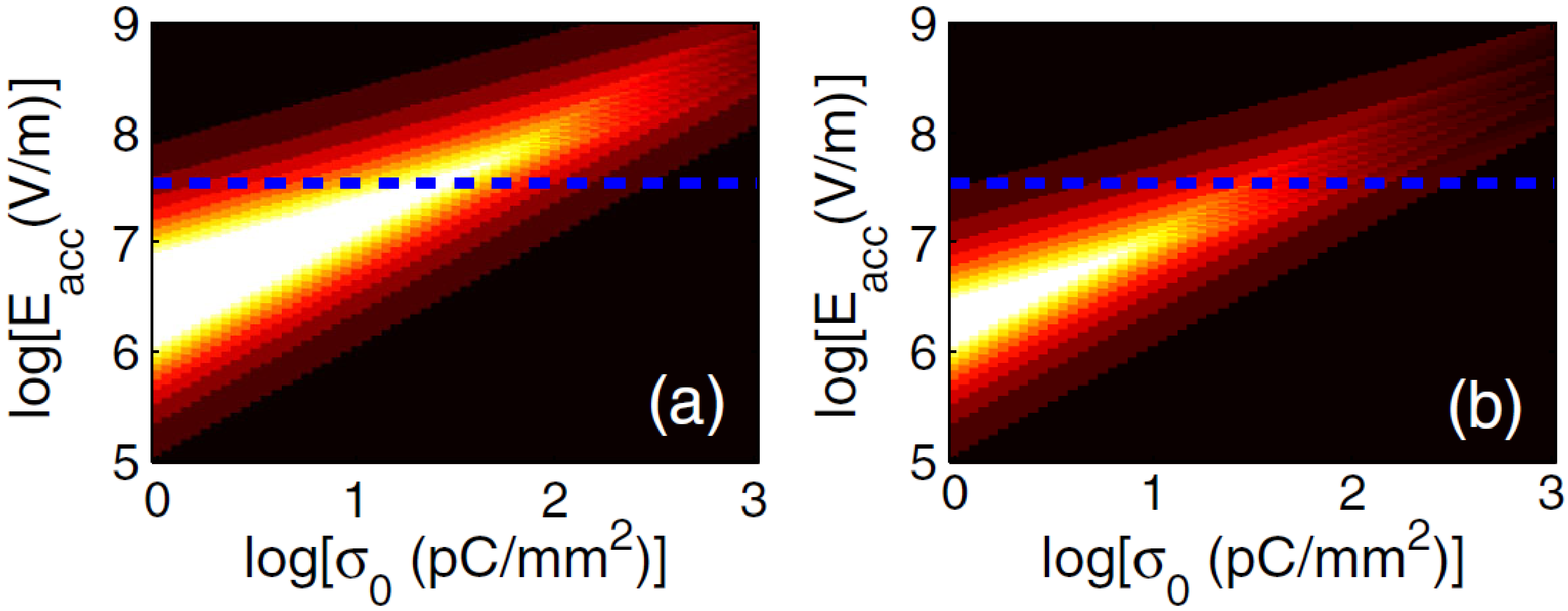

FIG. 1. Domain of existence of the blow-out regime (lighter colors) in the (σ_0, E_{acc}) parameter space for $\tau_l = 50$ fs (a) and $\tau_l = 200$ fs (b). The horizontal blue dashed lines correspond to $E_0 = 35$ MV/m. (This figure was adapted from Ref. [13].)

$\tau_l = 200\ fs$ could still support the blow-out scheme !

The A0 photoinjector setup and photocathode laser

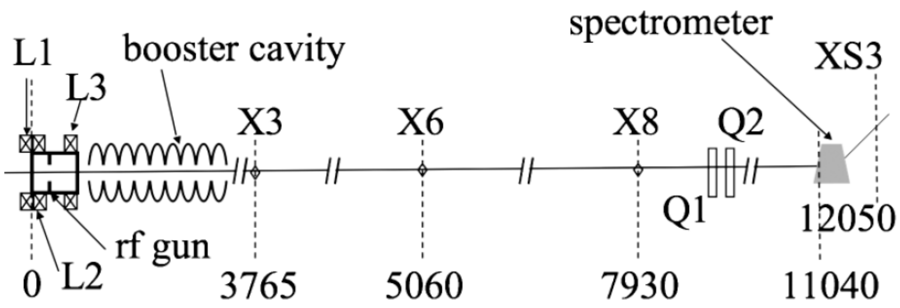

FIG. 2. Top view of the A0PI setup displaying elements pertinent to the present simulations and experiments. The "L" refers to solenoidal lenses, "X" to diagnostic stations (beam viewers and/or multislit masks location), and "Q" to quadrupole magnets. The distances are in mm and referenced to the photocathode surface.

TABLE I. Nominal settings for the rf gun, booster cavity, and the photocathode UV laser.

Parameter	Value	Units
Laser injection phase[a]	45 ± 5	rf deg
Laser radius on cathode	[0.3,2]	mm
Laser rms pulse duration	<200	fs
Bunch charge	[100–700]	pC
E_z on cathode (E_0)	33.7 ± 0.2	MV/m
peak B_z[b] (L2, L3)	$(0.158 - 0.041)$	T
Booster cavity gradient	~12.0	MV/m
Booster cavity phase[c]	$[-60–60]$	rf deg

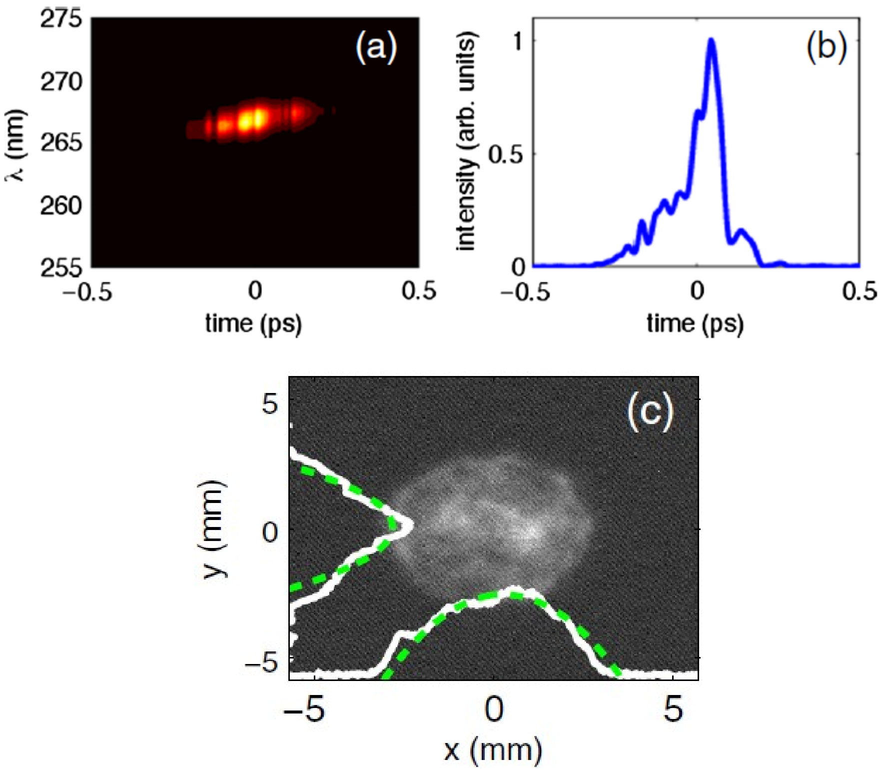

FIG. 3. Characterization of the UV laser pulse. Measured spectrogram (a) using a polarization-gate implementation of the frequency-resolved optical gating (FROG) technique and reconstructed temporal distribution (b) of the UV pulse (the inferred rms UV pulse duration is 122 fs). Typical transverse spatial distribution of the UV laser pulse on the photocathode (c) with associated projection (white traces) and parabolic fits (green traces).

Numerical simulations: emission time modelling

In order to take into account the finite emission time in ASTRA simulations, the data shown in Fig.4 (a) was parameterized with the following function → $\Lambda(t) = a_1 e^{-t/\tau_1} + a_2 e^{-t/\tau_2}$

The temporal charge distribution during the photoemission process

$Q(t) = \int_{-\infty}^{\infty} Q_0(t')\Lambda(t-t')dt'$, where $Q_0(t')$ is a Gaussian charge distribution with duration given by drive-laser pulse duration σ_t.

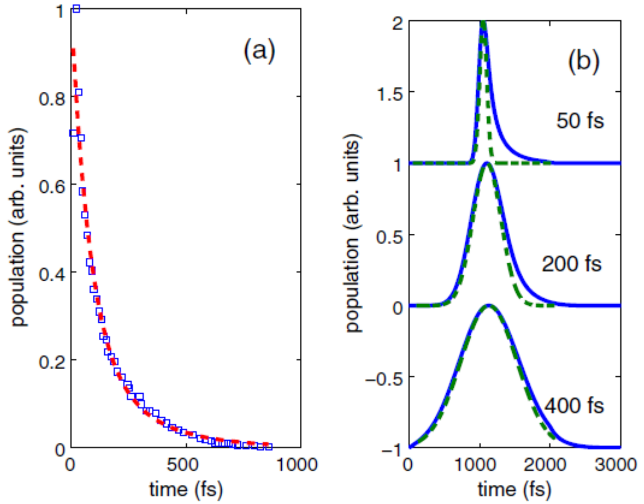

FIG. 4. Monte Carlo simulation (squares) taken from Ref. [39] and parametrization (dashed line) of the electron transit time from an initial Dirac-like laser excitation (a). Impact of the slow response time on the photoemission profile (blue traces) for three different Gaussian-like laser profiles (green dashed traces) of indicated rms duration (b). The traces in plot (b) are vertically offset for clarity. Larger time ordinates correspond to the bunch tail.

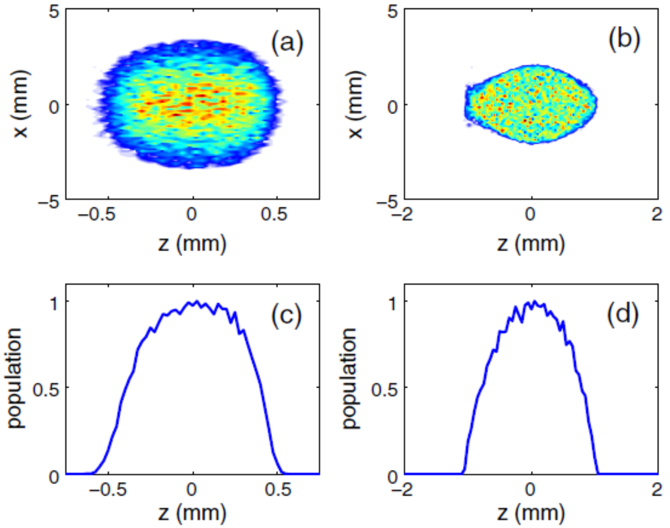

FIG. 5. Simulated spatiotemporal distribution (z, x) at $s = 0.47$ m (a) and $s = 3.77$ m (b) (corresponding to X3 screen) w.r.t. to the photocathode and associated longitudinal charge distributions [(c) and (d), respectively]. The charge is 250 pC and the rms laser transverse size is $\sigma_c = 1$ mm. In these plots the tail of the bunch is at $z > 0$.

Photoemission process was simulated using emission profile described above. Result in Fig.5, **showing that for low charges of ~250pC, A0 can operate in blow-out regime.**

Numerical simulations: introducing figure of merit

To investigate the domain of existence of blow-out regime in (σ_0, E_0) parameter space, a figure of merit (linearity of phase space) was introduced to quantify the ellipsoidal character of the bunch.

$$\mathcal{D}_u = \frac{1}{N}\sum_{i=1}^{N} d_{u,i}, \qquad \text{with } d_{u,i} = \frac{|u'_i - m_u u_i - q_u|}{\sqrt{1+m_u^2}}$$

where summation is performed over the number of macroparticles in bunch. (u,u') are trace space coordinates, m_u and q_u are slope and intersect of the linear regression of particle distribution in (u,u')

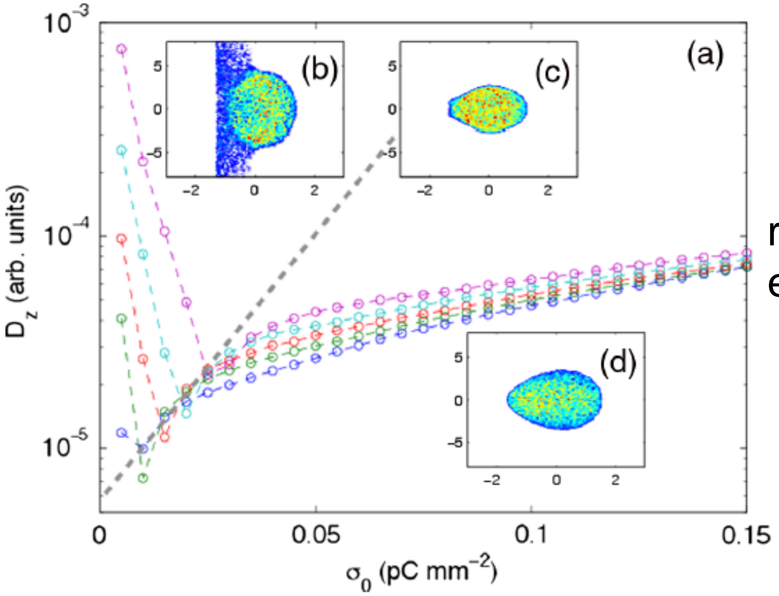

FIG. 7. Computed $\mathcal{D}_z$ metric [see Eq. (4)] (a) for bunch charges of 100, 250, 500, 1000, and 2000 pC (shown respectively as blue, green, red, cyan, and magenta symbols) as a function of cathode surface density σ_0. The gray line indicates loci of minimum $\mathcal{D}_z$ and the insets (b), (c), and (d) show typical spatiotemporal distributions simulated for the three regimes delineated by the gray line; see text for details. The simulation results are evaluated at the location of X3 in Fig. 2. The insets plot horizontal (respectively vertical) axes corresponding to z (respectively y) both in units of mm.

results obtained for 200fs emission time profile

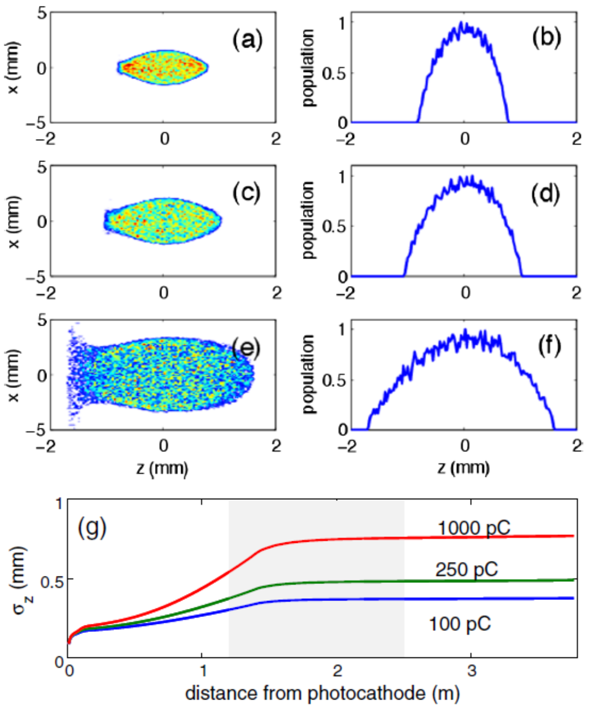

FIG. 6. Simulated spatiotemporal distribution (z, x) (left column) and associated longitudinal charge distribution (right column) simulated at X3 ($s = 3.77$ m) for three cases of charges 100 [(a), (b)], 250 [(c), (d)], and 1000 pC [(e), (f)]. In these plots the tail of the bunch is at $z > 0$. Plot (g) illustrates the rms bunch length evolution along the beam line up to $z = 3.77$ m (location of X3) for the three cases of bunch charge. The shaded area in plot (g) indicates the location of the booster cavity. The rms laser transverse size is kept constant to $\sigma_c = 1$ mm for the three cases of charges.

SC driven bunch length expansion is strongly suppressed once the bunch is accelerated by the booster cavity.

Experimental results and analyses I

- Transverse beam density

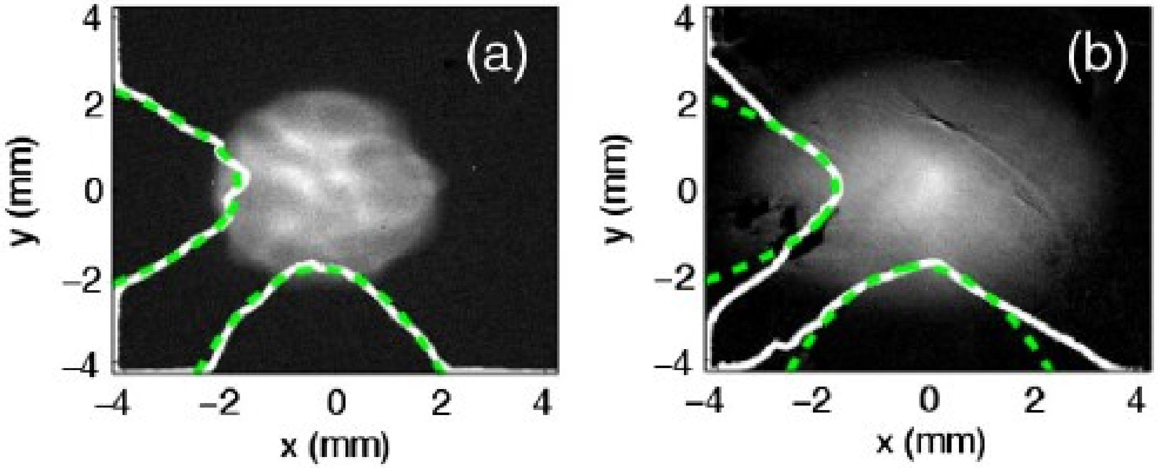

FIG. 8. Examples of measured spatial (*x*, *y*) distribution and associated projections (white solid lines) with parabolic fit (green dash lines). Images (a) and (b) respectively correspond to the beam being photoemitted using the ultrashort Ti:Sp and the picosecond Nd:YLF laser systems. The beam density is measured at the Ce:YAG screen X6 (see Fig. 2) for $Q \simeq 250 \pm 50$ pC.

Comparison of beam images at X6 (spatial distributions) crated with ultra-short (~200fs) and picosecond (~3ps) laser systems.

Experimental results and analyses II

> Longitudinal phase-space chirp

LPS correlation downstream the booster running at off-crest:

$$\langle z\delta\rangle = \langle z_0\delta_0\rangle \frac{\bar{E}_0}{\bar{E}} - \frac{eV}{\bar{E}} k \langle z_0^2\rangle \sin\varphi,$$

LPS chirp: $$\mathcal{C} \equiv \frac{\langle z_0\delta_0\rangle}{\langle z_0^2\rangle} = \frac{eV}{\bar{E}_0} k \sin\varphi_0.$$

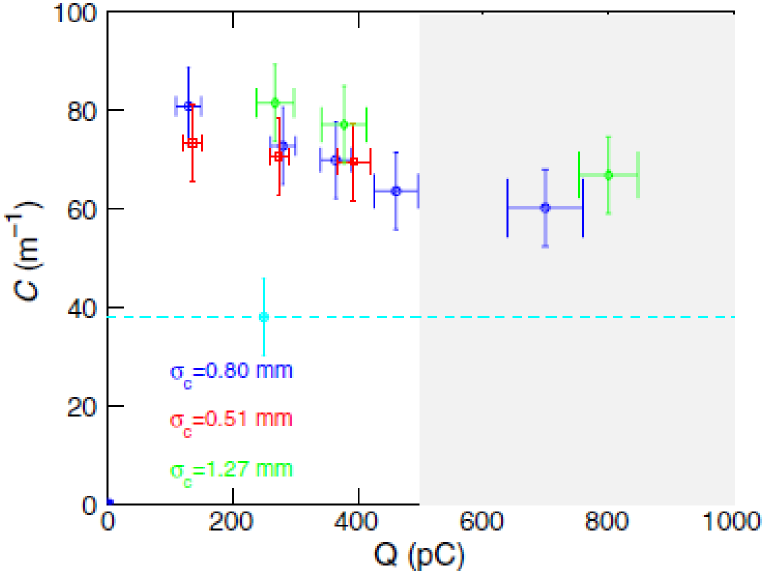

FIG. 10. Measured longitudinal-phase-space chirp $\mathcal{C} \equiv \langle z_0\delta_0\rangle/\langle z_0^2\rangle$ as a function of charge for three cases of laser transverse rms size σ_c on the photocathode surface. The horizontal dashed line represents the nominal chirp when the 3-ps-long Nd:YLF laser is used for photoemission. The shaded area represents the domain where the parabolic character of the temporal distribution was observed to be distorted and is consequently associated to a regime where a uniformly filled-ellipsoid bunch is not realized. The chirp associated to the electron bunch produced with the Nd:YLF laser was found to be independent of the charge and only one measurement (performed for $Q = 250$ pC) is shown.

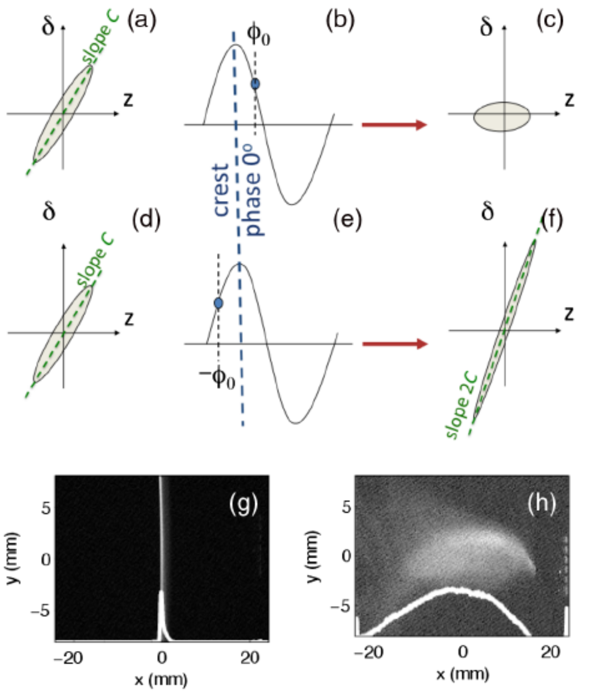

FIG. 9. Principle of measurement of the LPS chirp [(a), (b), and (c)] and bunch length [(d), (e), and (f)] measurements. The left [plots (a), (d)], middle [plots (b), (e)], and right [plots (c), (f)] columns show respectively the initial LPS, the location of the bunch (shown as a blue circle) w.r.t. the accelerating voltage, and the final LPS. The images (g) and (h) respectively show an example distribution measured at the XS3 location for minimum-energy-spread and off-crest phase settings; see text for details. In these latter images the horizontal axis corresponds to the energy-dispersed direction [x[mm] $\simeq 317\delta$ where δ is the unitless fractional momentum spread].

Fig.9 g) and h) show the momentum distribution at XS3 location for min energy spread and off-crest (2C) phase settings.

Experimental results and analyses III

> Spatiotemporal and current distributions

Zero-phasing technique used for the measurements:

- Chirped bunch (off-crest phase in the booster) + horizontally dispersed beam in a spectrometer + proper tuning of Q1 and Q2 quadrupoles

$$x_f = R_{11}x + R_{12}x' + \eta\tilde{\delta}_0 + 2\eta\mathcal{C}z_0$$

For the lowest measured charge (~130pC), the measured rms bunch length is ~1.6 ps → ~10-fold increase compared to initial bunch rms duration.

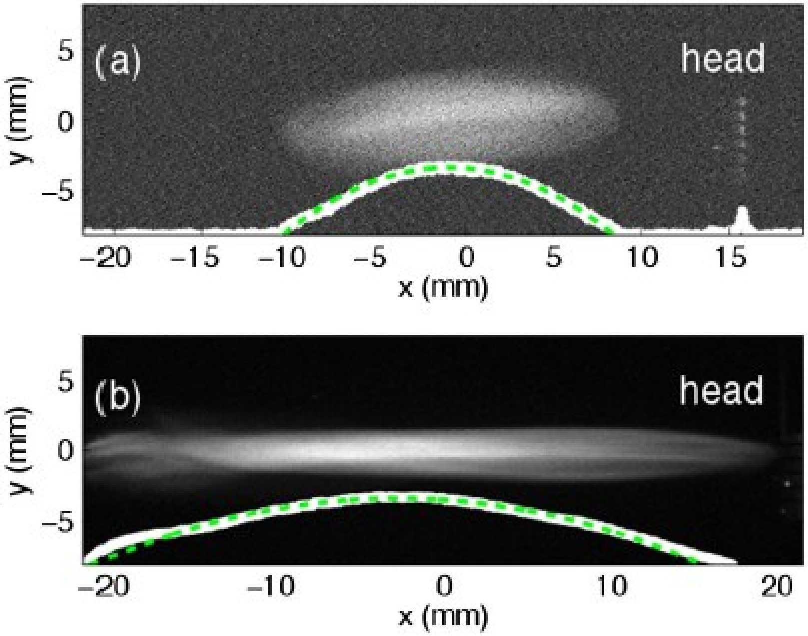

FIG. 11. Measured spatiotemporal ($x \propto t, y$) distribution and associated projections (white solid lines) with parabolic fit (green dash lines). The beam density is measured at the Ce:YAG screen XS3 (see Fig. 2) for $Q = 100 \pm 20$ pC (a) and $Q = 480 \pm 30$ pC (b).

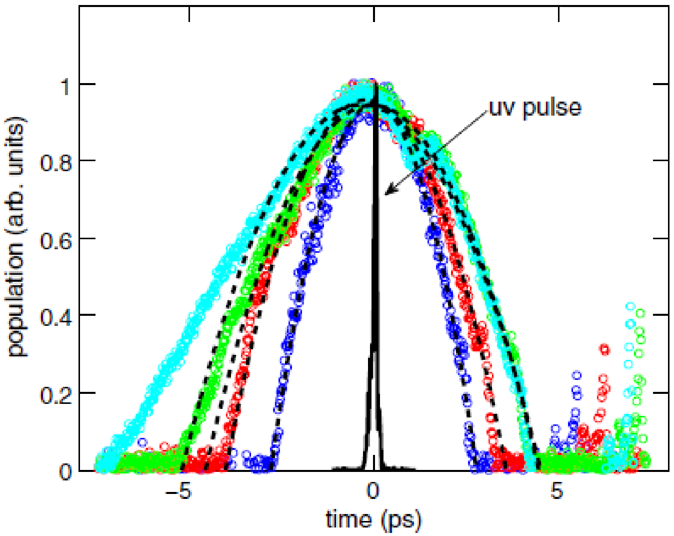

FIG. 12. Measured peak-normalized temporal profiles for $Q \simeq$ 130, 280, 460, and 700 pC (respectively shown as blue, red, green, and cyan circles), compared with the measured uv laser temporal profile (black solid trace). The dashed lines represent the results of parabolic fits to the measured profiles. The head of the bunch corresponds to $t > 0$.

Experimental results and analyses IV

- Electron bunch length as function of charge
- Electron beam transverse emittance for 250pC charge

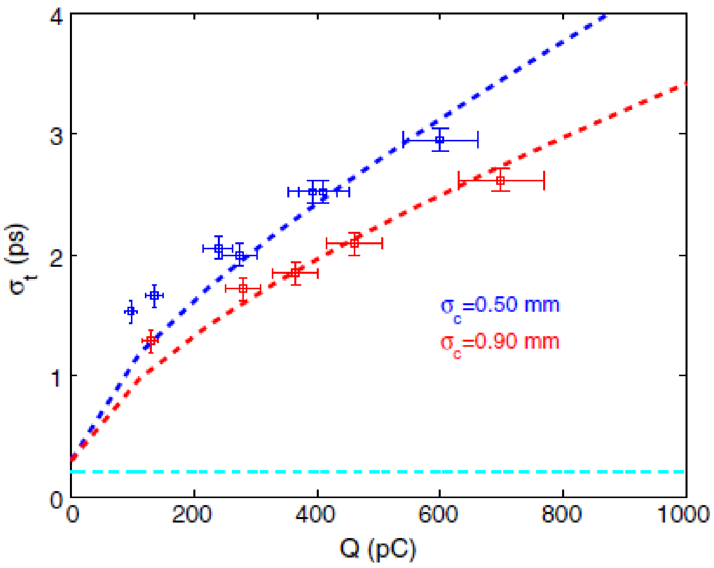

FIG. 13. Measured rms electron-bunch duration (symbols) as a function of charge for two cases of laser transverse spot size σ_c on the photocathode. The dashed red and blue lines are the corresponding simulations carried with ASTRA. The dashed cyan line represent the UV laser pulse duration.

$$\varepsilon_{\min} \propto \sqrt{\frac{Q}{E_0}}$$

Estimated achievable emittance in blow-out regime

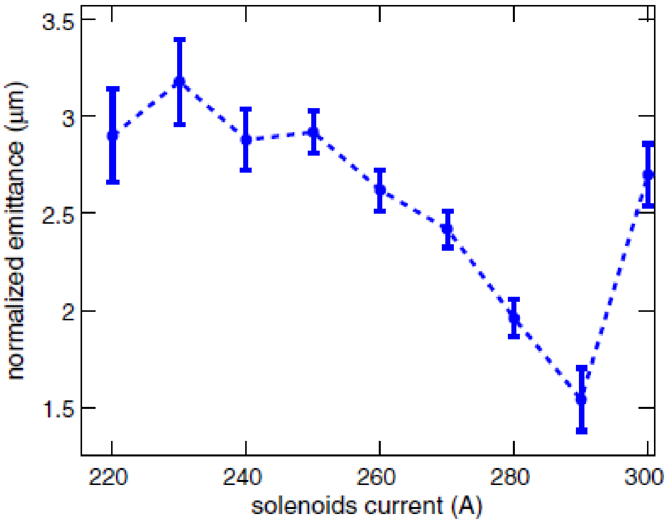

FIG. 14. Normalized transverse horizontal emittance measured as a function of the current setting of the solenoidal lenses (shown as L1, L2, and L3 in Fig. 2) for $Q = 266 \pm 25$ pC.

Direct shaping the laser profile to follow an ellipsoidal distribution would be more effective when improvement of transverse emittance is desired !

Summary

\+ Experimentally demonstrated the production of uniformly filled ellipsoidal bunch in an L-band rf photoinjector with Cs_2Te cathode using ultra-short laser pulse

\+ The bunch ellipsoidal character is preserved after acceleration to ~14 MeV and charges up to ~0.5 nC

For the future more precise LPS characterization is expected by using a transverse deflecting cavity

\- No comparison of experimental results with the simulations

\- Transverse emittance value still too big